

Zee model in a non-holomorphic modular A_4 symmetry

Takaaki Nomura^{1,*} and Hiroshi Okada^{2,†}

¹*College of Physics, Sichuan University, Chengdu 610065, China*

²*Department of Physics, Henan Normal University, Xinxiang 453007, China*

(Dated: December 25, 2024)

We study a Zee model in a non-holomorphic modular A_4 flavor symmetry in which we find good predictions in both the cases of normal and inverted hierarchy. Parameter reduction on neutrino sector occurs due to large mass hierarchies between charged-leptons mass eigenvalues and new singly-charged bosons in addition to this flavor symmetry. As a result, we have two complex free parameters including modulus τ . We show several predictions in terms of verifiable observables such as Dirac CP, Majorana phases, sum of the neutrino masses, and the effective mass for neutrino double beta decay in addition to demonstrating allowed regions for our input parameters.

PACS numbers:

arXiv:2412.18095v1 [hep-ph] 24 Dec 2024

*Electronic address: nomura@scu.edu.cn

†Electronic address: hiroshi3okada@htu.edu.cn

I. INTRODUCTION

Searching for plausible scenario for neutrino sector would be important to understand particle physics beyond the standard model (BSM). Since supersymmetry(SUSY) is unlikely to exist at low energy scale that can reach at our current experiments \sim TeV, it would be promising to work on non-supersymmetric theory as a first step. Recently, a group of "Qu" and "Ding" successfully constructed a non-holomorphic modular flavor symmetries that can still work on non-supersymmetric theory [1]. Thanks to their big efforts, more varieties of scenarios have been taken in consideration [2–5]. Zee model [6] is one of the attractive scenarios to generate the non-vanishing neutrino masses radiatively since it is expected to be detected at TeV scale.¹

In this paper, we apply the non-holomorphic modular A_4 flavor symmetry for Zee model and construct the model as minimum as possible. Thanks to non-holomorphic features, we have drastically reduced our free parameter compared to our previous scenario under the holomorphic modular A_4 symmetry [8]. As a result, we obtain good predictions in terms of verifiable observables such as Dirac CP, Majorana phases, sum of the neutrino masses, and the effective mass for neutrino double beta decay for both the cases of normal and inverted hierarchy performing χ square analysis.

This paper is organized as follows. In Sec. II, we review our minimum Zee model constructing the renormalizable valid Lagrangian, Higgs potential, charged-lepton mass matrix, and active neutrino mass matrix. Then, we numerically fix the Higgs masses and mixings so that our analysis makes it simpler. After discussing the charged-lepton sector, we formulate the neutrino sector. In Sec. III, we perform χ square analysis and show some predictions for normal and inverted hierarchies. We have conclusions and discussion in Sec. IV.

	Leptons		Bosons		
	\overline{L}_L	ℓ_R	Φ	Φ'	S^-
$SU(2)_L$	2	1	2	2	1
$U(1)_Y$	$-\frac{1}{2}$	1	$\frac{1}{2}$	$\frac{1}{2}$	-1
A_4	3	3	1	1	1
$-k_I$	-1	+1	0	-2	+2

TABLE I: Field contents and their charge assignments in Zee model under $SU(2)_L \times U(1)_Y \times A_4$ where $-k_I$ is the number of modular weight.

¹ We should also mention Ma model that is the first neutrino model at one-loop including dark matter candidate [7] although Zee model does not have dark matter.

II. MODEL SETUP

The field contents in our model setup is exactly the same as Zee model, i.e. two Higgs doublets Φ , Φ' plus singly-charged boson S^- are introduced. The charge assignments under modular A_4 are shown in Tab I. The assignments are chosen so that the model is as minimum as possible where we define $\overline{L}_L \equiv [\overline{L}_{L_e}, \overline{L}_{L_\mu}, \overline{L}_{L_\tau}]^T$, $\ell_R \equiv [e_R, \mu_R, \tau_R]^T$ as flavor eigenstates. Then, the renormalizable Lagrangian for lepton sector is found as follows:

$$\begin{aligned}
-\mathcal{L}_\ell = & a_\ell [\overline{L}_{L_e} e_R + \overline{L}_{L_\mu} \tau_R + \overline{L}_{L_\tau} \mu_R] \Phi \\
& + b_\ell [y_1(2\overline{L}_{L_e} e_R - \overline{L}_{L_\mu} \tau_R - \overline{L}_{L_\tau} \mu_R) + y_2(2\overline{L}_{L_\mu} \mu_R - \overline{L}_{L_e} \tau_R - \overline{L}_{L_\tau} e_R) \\
& + y_3(2\overline{L}_{L_\tau} \tau_R - \overline{L}_{L_e} \mu_R - \overline{L}_{L_\mu} e_R)] \Phi \\
& + c_\ell [y_1(\overline{L}_{L_\mu} \tau_R - \overline{L}_{L_\tau} \mu_R) + y_2(-\overline{L}_{L_e} \tau_R + \overline{L}_{L_\tau} e_R) + y_3(\overline{L}_{L_e} \mu_R - \overline{L}_{L_\mu} e_R)] \Phi \\
& + a'_\ell [f_1(2\overline{L}_{L_e} e_R - \overline{L}_{L_\mu} \tau_R - \overline{L}_{L_\tau} \mu_R) + f_2(2\overline{L}_{L_\mu} \mu_R - \overline{L}_{L_e} \tau_R - \overline{L}_{L_\tau} e_R) \\
& + f_3(2\overline{L}_{L_\tau} \tau_R - \overline{L}_{L_e} \mu_R - \overline{L}_{L_\mu} e_R)] \Phi' \\
& + b'_\ell [f_1(\overline{L}_{L_\mu} \tau_R - \overline{L}_{L_\tau} \mu_R) + f_2(-\overline{L}_{L_e} \tau_R + \overline{L}_{L_\tau} e_R) + f_3(\overline{L}_{L_e} \mu_R - \overline{L}_{L_\mu} e_R)] \Phi' \\
& + a_s [y_1(\overline{L}_{L_\mu} L_{L_\tau}^C - \overline{L}_{L_\tau} L_{L_\mu}^C) + y_2(-\overline{L}_{L_e} L_{L_\tau}^C + \overline{L}_{L_\tau} L_{L_e}^C) + y_3(\overline{L}_{L_e} L_{L_\mu}^C - \overline{L}_{L_\mu} L_{L_e}^C)] S^- + h.c.,
\end{aligned} \tag{II.1}$$

where we define $Y_3^{(0)} = [y_1, y_2, y_3]$ and $Y_3^{(2)} = [f_1, f_2, f_3]$ [1].

A. Higgs sector

The Higgs sector of the model is the same as the one in the Zee model. The relevant scalar sector is given by

$$\begin{aligned}
\mathcal{V} = & \mu_1^2 |\Phi'|^2 + \mu_2^2 |\Phi|^2 - (\mu_3^2 \Phi^\dagger \Phi' + h.c.) + \mu_S^2 |S^-|^2 + \mu(\Phi^T \cdot \Phi') S^- \\
& + \frac{\lambda_1}{2} |\Phi'|^4 + \frac{\lambda_2}{2} |\Phi|^4 + \lambda_S |S|^4 + \lambda_3 |\Phi|^2 |\Phi'|^2 + \lambda_4 |\Phi^\dagger \Phi'|^2 + \frac{\lambda_5}{2} ((\Phi^\dagger \Phi')^2 + h.c.) \\
& + \lambda_{\Phi S} |\Phi|^2 |S|^2 + \lambda_{\Phi' S} |\Phi'|^2 |S|^2,
\end{aligned} \tag{II.2}$$

where all the above parameters except μ_2^2 , λ_2 , and μ include $1/(\tau - \tau^*)^{k_I}$ factor, and μ_3^2 and λ_5 respectively contain modular form $Y_1^{(2)}$ and $Y_1^{(4)}$ in order to be invariant under the modular A_4 symmetry; these extra factors are absorbed into the parameters after τ value is fixed. Here we

introduce the Higgs basis (H, H') as

$$\begin{pmatrix} \Phi' \\ \Phi \end{pmatrix} = \begin{pmatrix} c_\beta & -s_\beta \\ s_\beta & c_\beta \end{pmatrix} \begin{pmatrix} H \\ H' \end{pmatrix} \quad (\text{II.3})$$

where $c_\beta(s_\beta) \equiv \cos\beta(\sin\beta)$ with mixing angle β defined by the ratio of vacuum expectation values (VEVs) as $\tan\beta = \langle\Phi\rangle/\langle\Phi'\rangle$. Then H and H' are written as follows:

$$H = \begin{pmatrix} w^+ \\ \frac{v+\tilde{h}+iz}{\sqrt{2}} \end{pmatrix}, \quad H' = \begin{pmatrix} h'^+ \\ \frac{\tilde{h}'+iA}{\sqrt{2}} \end{pmatrix}, \quad (\text{II.4})$$

where $v \approx 246$ GeV is the VEV in the Higgs basis after the spontaneous symmetry breaking, z is absorbed by the neutral gauge boson of the SM Z , and w^+ is absorbed by the charged gauge boson of the SM W^+ . As in the two Higgs doublet model (THDM) the mass eigenstates for the CP even physical bosons are written by

$$\begin{pmatrix} \tilde{h} \\ \tilde{h}' \end{pmatrix} = \begin{pmatrix} c_{\alpha-\beta} & -s_{\alpha-\beta} \\ s_{\alpha-\beta} & c_{\alpha-\beta} \end{pmatrix} \begin{pmatrix} H \\ h \end{pmatrix}, \quad (\text{II.5})$$

where the mixing angle α can be expressed in terms of parameters in the potential, and mass eigenvalues are m_h and m_H . In our analysis, we consider the alignment limit of $\sin(\beta - \alpha) = 1$ to avoid experimental constraints associated with Higgs boson measurements. For simplicity we also choose parameters in the potential so that $\tan\beta \gg 1$ and $\Phi \simeq H$ is the SM like Higgs field. Thus we approximate as $\langle\Phi\rangle \simeq v/\sqrt{2}$ and neglect the SM fermion mass terms from VEV of $\Phi' \simeq H'$.

The mass eigenvalue of CP odd one is given by

$$m_A^2 = \frac{\mu_3^2}{s_\beta c_\beta} - v^2 \lambda_5. \quad (\text{II.6})$$

The mass matrix of singly-charged bosons is given by

$$M_C^2 = \begin{pmatrix} \frac{\mu_3^2}{s_\beta c_\beta} - \frac{v^2}{2}(\lambda_4 + \lambda_5) & \frac{\mu v}{\sqrt{2}} \\ \frac{\mu v}{\sqrt{2}} & \mu_S^2 + \frac{v^2 s_\beta^2}{2} \lambda_{\Phi S} + \frac{v^2 c_\beta^2}{2} \lambda_{\Phi' S} \end{pmatrix}. \quad (\text{II.7})$$

Here, we presume that the singly-charged bosons are almost diagonal assuming $\mu \ll v$. Thus, we consider that the neutrino mass matrix is found through the mass insertion approximation as shown below. Therefore,

$$m_{h'}^2 \approx \frac{\mu_3^2}{s_\beta c_\beta} - \frac{v^2}{2}(\lambda_4 + \lambda_5), \quad (\text{II.8})$$

$$m_s^2 \approx \mu_S^2 + \frac{v^2 s_\beta^2}{2} \lambda_{\Phi S} + \frac{v^2 c_\beta^2}{2} \lambda_{\Phi' S}. \quad (\text{II.9})$$

B. Charged-lepton mass matrix

After the spontaneous electroweak symmetry breaking, the charged-lepton mass matrix M_e is given by

$$M_e = \frac{v}{\sqrt{2}} \left[a_e \begin{pmatrix} 1 & 0 & 0 \\ 0 & 0 & 1 \\ 0 & 1 & 0 \end{pmatrix} + b_e \begin{pmatrix} 2y_1 & -y_3 & -y_2 \\ -y_3 & 2y_2 & -y_1 \\ -y_2 & -y_1 & 2y_3 \end{pmatrix} + c_e \begin{pmatrix} 0 & y_3 & -y_2 \\ -y_3 & 0 & y_1 \\ y_2 & -y_1 & 0 \end{pmatrix} \right], \quad (\text{II.10})$$

where a_e, b_e, c_e are real without loss of generality. Then, the charged-lepton mass matrix is diagonalized by a bi-unitary mixing matrix as $D_e \equiv \text{diag}(m_e, m_\mu, m_\tau) = V_{eL}^\dagger M_e V_{eR}$. These three parameters are used in order to fit the mass eigenvalues of charged-leptons by solving the following three relations:

$$\text{Tr}[M_e M_e^\dagger] = |m_e|^2 + |m_\mu|^2 + |m_\tau|^2, \quad (\text{II.11})$$

$$\text{Det}[M_e M_e^\dagger] = |m_e|^2 |m_\mu|^2 |m_\tau|^2, \quad (\text{II.12})$$

$$(\text{Tr}[M_e M_e^\dagger])^2 - \text{Tr}[(M_e M_e^\dagger)^2] = 2(|m_e|^2 |m_\mu|^2 + |m_\mu|^2 |m_\tau|^2 + |m_e|^2 |m_\tau|^2). \quad (\text{II.13})$$

C. Active neutrino mass matrix

The active neutrino mass matrix is given at one-loop level via the following Lagrangian in terms of mass eigenstates of charged-leptons and singly-charged-bosons:

$$a' \bar{\nu}_L f V_{eR} \ell_R h'^+ + a_s \bar{\ell}_L V_{eL}^\dagger y^T \nu_L^c S^- + \frac{\mu v}{\sqrt{2}} h'^- S^+ + \text{h.c.}, \quad (\text{II.14})$$

where f and y are respectively given by

$$f = \begin{pmatrix} 2f_1 & -f_3 & -f_2 \\ -f_3 & 2f_2 & -f_1 \\ -f_2 & -f_1 & 2f_3 \end{pmatrix} + \tilde{b}'_k \begin{pmatrix} 0 & f_3 & -f_2 \\ -f_3 & 0 & f_1 \\ f_2 & -f_1 & 0 \end{pmatrix}, \quad (\text{II.15})$$

$$y = \begin{pmatrix} 0 & y_3 & -y_2 \\ -y_3 & 0 & y_1 \\ y_2 & -y_1 & 0 \end{pmatrix}. \quad (\text{II.16})$$

The neutrino mass matrix is found at one-loop level as follows:

$$(m_\nu)_{ij} \approx \frac{a_s a'}{(4\pi)^2} \frac{v\mu}{\sqrt{2}m_{h'}^2} \frac{\ln r}{1-r} \sum_{a=1} (F_{ja} m_{\ell_a} Y_{aj}^T + Y_{ia}^T m_{\ell_a} F_{aj}), \quad (\text{II.17})$$

where $r \equiv m_s^2/m_{h'}^2$, $F \equiv fV_{eR}$, $Y \equiv yV_{eL}^*$, and the loop function does not depend on the mass of charged-leptons since we assume $m_{e,\mu,\tau} \ll m_{h'}$, m_s . We define the overall factor as follows: $\kappa \equiv \frac{a_s a'}{(4\pi)^2} \frac{v\mu}{\sqrt{2}m_{h'}^2} \frac{\ln r}{1-r}$, therefore $m_\nu \equiv \kappa \tilde{m}_\nu$. Then, \tilde{m}_ν is diagonalized by a unitary matrix U_ν as $U_\nu^T \tilde{m}_\nu U_\nu = \tilde{D}_\nu$ with $\tilde{D}_\nu = \text{diag}[\tilde{D}_{\nu_1}, \tilde{D}_{\nu_2}, \tilde{D}_{\nu_3}]$, and the Pontecorvo-Maki-Nakagawa-Sakata unitary matrix U_{PMNS} is defined by $V_{eL}^\dagger U_\nu$. The observed atmospheric mass squared difference Δm_{atm}^2 is given by

$$\text{NH} : \Delta m_{atm}^2 = |\kappa|^2 (\tilde{D}_{\nu_3}^2 - \tilde{D}_{\nu_1}^2), \quad (\text{II.18})$$

$$\text{IH} : \Delta m_{atm}^2 = |\kappa|^2 (\tilde{D}_{\nu_2}^2 - \tilde{D}_{\nu_3}^2), \quad (\text{II.19})$$

where NH(IH) represents normal(inverted) hierarchy. The solar mass squared difference Δm_{sol}^2 is then given by

$$\Delta m_{sol}^2 = |\kappa|^2 (\tilde{D}_{\nu_2}^2 - \tilde{D}_{\nu_1}^2). \quad (\text{II.20})$$

Finally, the effective mass for neutrino double beta decay is given by

$$\langle m_{ee} \rangle = |\kappa| \left| \tilde{D}_{\nu_1} c_{12}^2 c_{13}^2 + \tilde{D}_{\nu_2} s_{12}^2 c_{13}^2 e^{i\alpha_{21}} + \tilde{D}_{\nu_3} s_{13}^2 e^{i(\alpha_{31} - 2\delta_{CP})} \right|. \quad (\text{II.21})$$

A current KamLAND-Zen data [9]. provides measured observable in future and its upper bound is given by $\langle m_{ee} \rangle < (36 - 156)$ meV at 90 % confidence level. The minimal cosmological model $\Lambda\text{CDM} + \sum D_\nu$ provides upper bound on $\sum D_\nu \leq 120$ meV [10, 11]. Moreover, recently combination of DESI and CMB data gives more stringent upper bound on this bound; $\sum D_\nu \leq 72$ meV [12].

III. NUMERICAL ANALYSIS

In this section we perform χ square analysis using data from NuFit6.0 [13] where we have adopt five reliable observables; three mixings, two mass square differences, for the analysis. The green points represents the interval of $1\sigma - 2\sigma$, yellow one $2\sigma - 3\sigma$, and red one $3\sigma - 5\sigma$. Our input parameter, which is complex, is randomly selected within the following range:

$$|\tilde{b}'_k| \in [10^{-5}, 10^5], \quad (\text{III.1})$$

where we work on the fundamental region of τ .

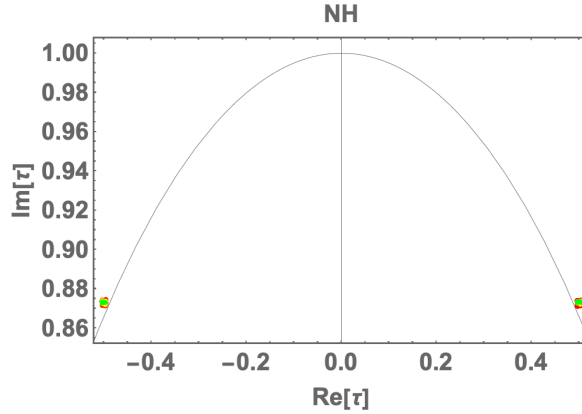


FIG. 1: Allowed region for real τ and imaginary τ in NH.

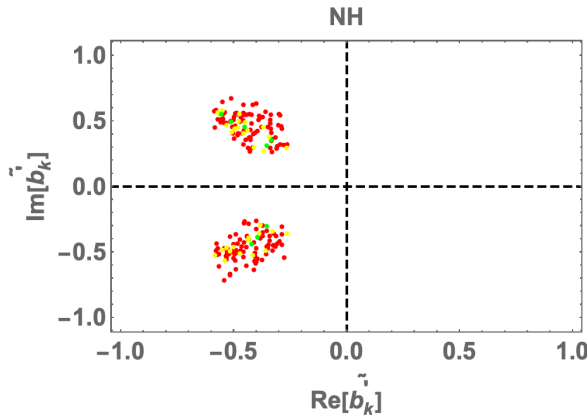


FIG. 2: Allowed region for real \tilde{b}'_k and imaginary \tilde{b}'_k in NH.

A. NH

In Fig. 1, we show the allowed region of τ , and find that the allowed region is located at nearby $\tau = e^{2\pi i/3}$. In Fig. 2, we also show the allowed region of \tilde{b}'_k , and find that the allowed region is about $\text{Re}[\tilde{b}'_k] = [-0.6, -0.2]$ and $|\text{Im}[\tilde{b}'_k]| = [0.2, 0.6]$.

In Fig. 3, we show the allowed region for δ_{CP} deg (left) and $\langle m_{ee} \rangle$ meV (right) in terms of $\sum D_\nu$ meV and find $\delta_{CP} = [30 - 100, 270 - 330]$ deg, $\sum D_\nu = [58 - 61]$ meV, and $\langle m_{ee} \rangle = [3.2 - 4.0]$ meV. The vertical magenta dotted line is upper bound on results of Planck+DESI [12] $\sum D_\nu \leq 72$ meV.

In Fig. 4, we show the allowed region for Majorana phases and find $\alpha_{31} = [240 - 280]$ deg and $\alpha_{21} = [60 - 120]$ deg. In addition, in Fig. 5, we show the allowed region for $\langle m_{ee} \rangle$ in terms of the lightest active neutrino mass in NH and find the lightest active neutrino mass to be $D_{\nu_1} = [0.2 - 1]$ meV.

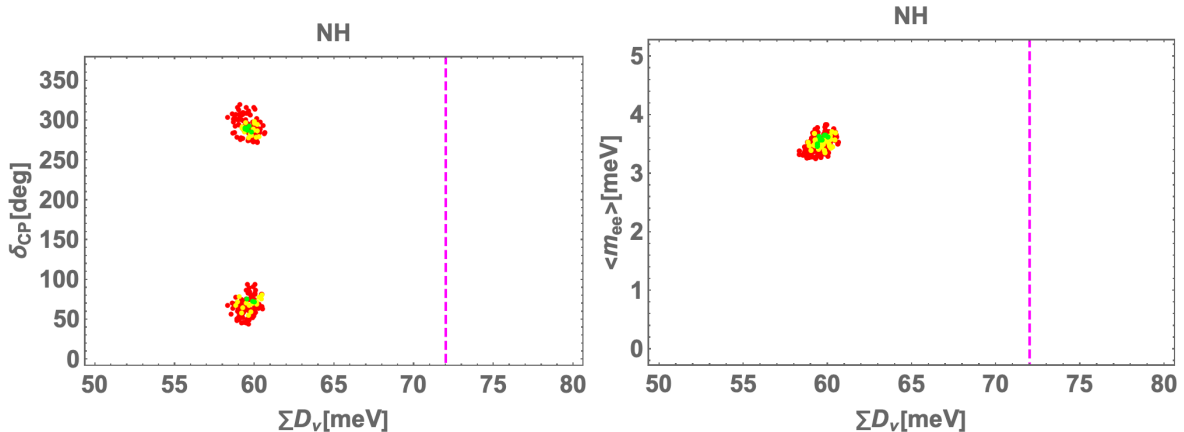


FIG. 3: Allowed regions for δ_{CP} deg (left) and $\langle m_{ee} \rangle$ meV (right) in terms of $\sum D_\nu$ meV in NH. The vertical magenta dotted line is upper bound on results of Planck+DESI [12] $\sum D_\nu \leq 72$ meV.

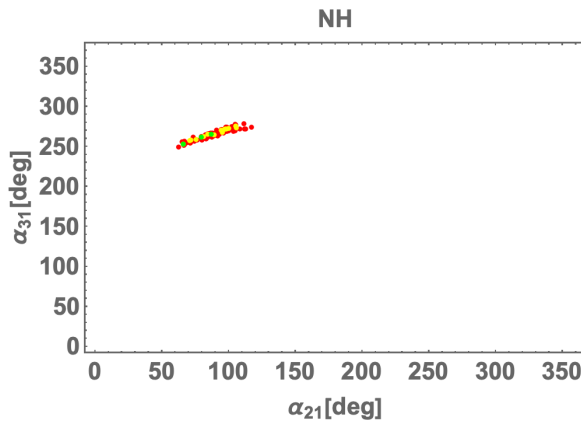


FIG. 4: Allowed region for Majorana phases meV in NH.

B. IH

In Fig. 6, we show the allowed region of τ , and find that the allowed region is located at nearby $|\text{Re}\tau| = [0.12 - 0.18]$ and $\text{Im}\tau = [1.95 - 2.10]$. In Fig. 7, we show the allowed region of \tilde{b}'_k , and find that the allowed region is about $\text{Re}[\tilde{b}'_k] \approx 1$ and $|\text{Im}[\tilde{b}'_k]| = [0.1 - 0.2]$.

In Fig. 8, we show the allowed region for δ_{CP} deg (left) and $\langle m_{ee} \rangle$ meV (right) in terms of $\sum D_\nu$ meV and find $\delta_{CP} = [120 - 250]$ deg, $\sum D_\nu = [102 - 108]$ meV, and $\langle m_{ee} \rangle = [12 - 20]$ meV. The vertical magenta and black dotted lines are respectively upper bound on results of Planck+DESI [12]; $\sum D_\nu \leq 72$ meV and the minimal cosmological model $\Lambda\text{CDM} + \sum D_\nu$ [10, 11]; $\sum D_\nu \leq 120$ meV. The horizontal gray dotted line is the lower bound on the KamLAND-Zen data 36 meV.

In Fig. 9, we show the allowed region for Majorana phases and find $\alpha_{31} = [0 - 10, 100 -$

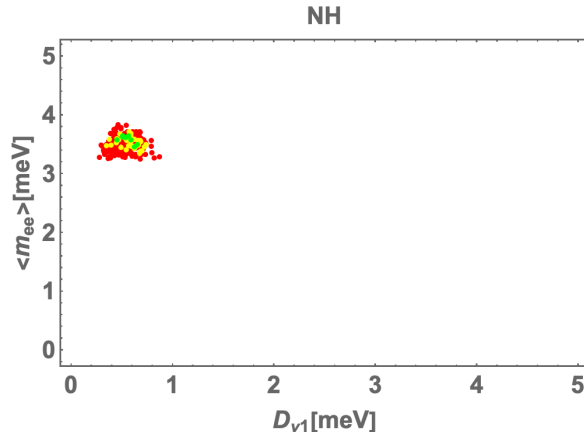


FIG. 5: Allowed region for $\langle m_{ee} \rangle$ in terms of the lightest active neutrino mass in NH.

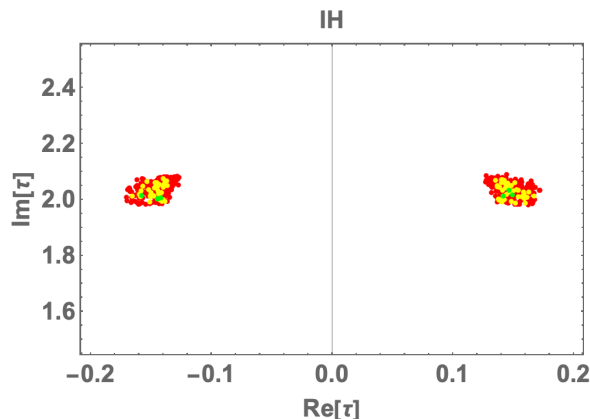


FIG. 6: Allowed region for real τ and imaginary τ in IH.

120, 240 – 360] deg and $\alpha_{21} = [140 - 210]$ deg. In Fig. 10, we show the allowed region for $\langle m_{ee} \rangle$ in terms of the lightest active neutrino mass in IH and find the lightest active neutrino mass to be $D_{\nu_3} = [4.5 - 6.2]$ meV.

IV. CONCLUSIONS AND DISCUSSIONS

We have investigated a Zee model applying a non-holomorphic modular A_4 symmetry, and we have obtained unique and sharp predictions for each of the normal and inverted hierarchy. This is because we have only two parameters in the neutrino sector including modulus τ due to appropriately assuming that the masses of charged-leptons are negligibly less than the masses for singly charged bosons.

Before closing this paper, we mention the constraints of Yukawa couplings f and y . These main constraints come from lepton/hadron universalities which are induced at tree level and charged

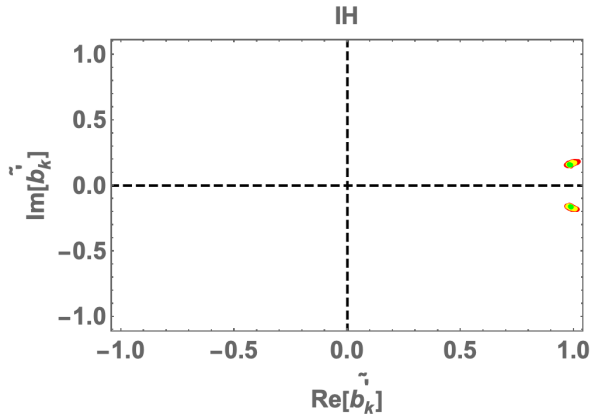


FIG. 7: Allowed region for real \tilde{b}'_k and imaginary \tilde{b}'_k in IH.

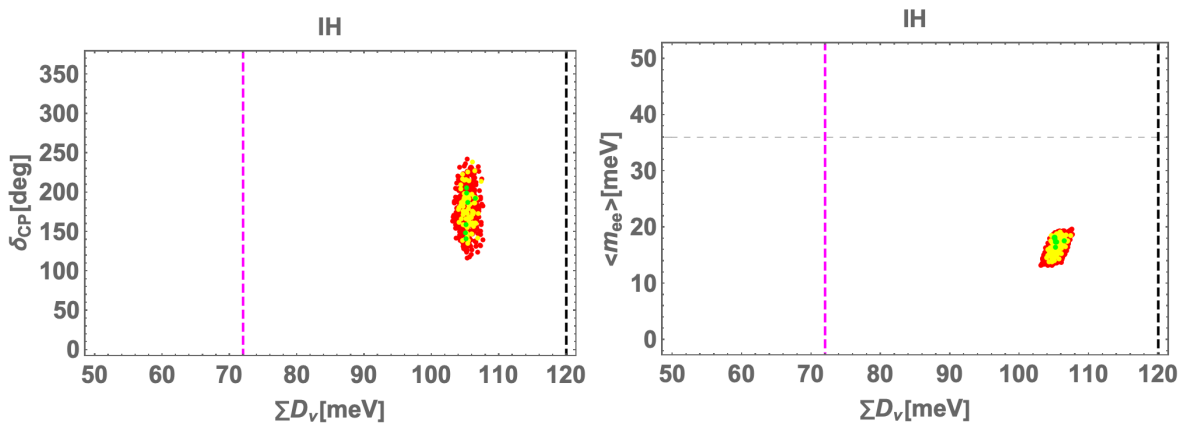


FIG. 8: Allowed regions for δ_{CP} deg (left) and $\langle m_{ee} \rangle$ meV (right) in terms of $\sum D_\nu$ meV in IH. The vertical magenta and black dotted lines are respectively upper bound on results of Planck+DESI [12]; $\sum D_\nu \leq 72$ meV and the minimal cosmological model $\Lambda\text{CDM} + \sum D_\nu$ [10, 11]; $\sum D_\nu \leq 120$ meV. The horizontal gray dotted line is lower bound on KamLAND-Zen data 36 meV.

lepton flavor violations which are induced at one-loop level [14–16]. Even when we consider these bounds, it is totally safe if we take these Yukawa couplings are 0.01 in case of $m_s \sim m_{h'} = 1$ TeV. This value is easily achieved by adjusting the overall factor a' and a_s , which are parts of κ . Although κ is fixed to fit the atmospheric mass squared difference, κ can still maintain the fit value due to changing μ and r .

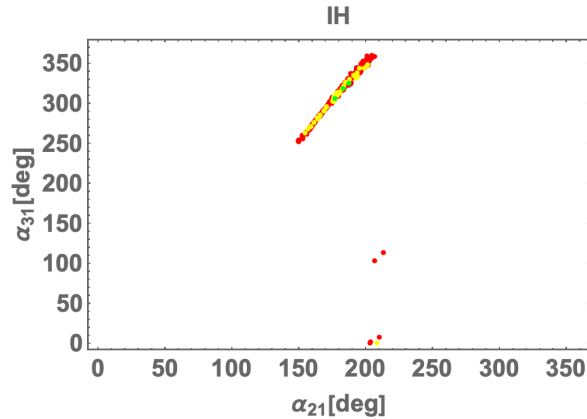


FIG. 9: Allowed region for Majorana phases meV in IH.

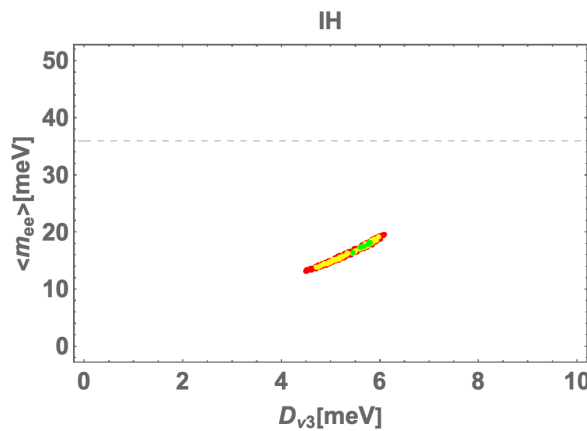


FIG. 10: Allowed region for $\langle m_{ee} \rangle$ in terms of the lightest active neutrino mass in IH.

Acknowledgments

The work was supported by the Fundamental Research Funds for the Central Universities (T. N.).

-
- [1] B.-Y. Qu and G.-J. Ding, JHEP **08**, 136 (2024), 2406.02527.
 - [2] G.-J. Ding, J.-N. Lu, S. T. Petcov, and B.-Y. Qu (2024), 2408.15988.
 - [3] C.-C. Li, J.-N. Lu, and G.-J. Ding (2024), 2410.24103.
 - [4] T. Nomura and H. Okada (2024), 2408.01143.
 - [5] T. Nomura, H. Okada, and O. Popov, Phys. Lett. B **860**, 139171 (2025), 2409.12547.
 - [6] A. Zee, Phys. Lett. B **93**, 389 (1980), [Erratum: Phys.Lett.B 95, 461 (1980)].
 - [7] E. Ma, Phys. Rev. D **73**, 077301 (2006), hep-ph/0601225.

- [8] T. Nomura, H. Okada, and Y.-h. Qi (2021), 2111.10944.
- [9] S. Abe et al. (KamLAND-Zen) (2024), 2406.11438.
- [10] S. Vagnozzi, E. Giusarma, O. Mena, K. Freese, M. Gerbino, S. Ho, and M. Lattanzi, *Phys. Rev. D* **96**, 123503 (2017), 1701.08172.
- [11] N. Aghanim et al. (Planck), *Astron. Astrophys.* **641**, A6 (2020), [Erratum: *Astron. Astrophys.* 652, C4 (2021)], 1807.06209.
- [12] A. G. Adame et al. (DESI) (2024), 2404.03002.
- [13] I. Esteban, M. C. Gonzalez-Garcia, M. Maltoni, I. Martinez-Soler, J. a. P. Pinheiro, and T. Schwetz (2024), 2410.05380.
- [14] J. Herrero-Garcia, M. Nebot, N. Rius, and A. Santamaria, *Nucl. Phys. B* **885**, 542 (2014), 1402.4491.
- [15] H. Okada (2015), 1503.04557.
- [16] M. Lindner, M. Platscher, and F. S. Queiroz, *Phys. Rept.* **731**, 1 (2018), 1610.06587.